Supplementary Material for

Entanglement between two spatially separated atomic modes

Karsten Lange, Jan Peise, Bernd Lücke, Ilka Kruse, Giuseppe Vitagliano, Iagoba Apellaniz, Matthias Kleinmann, Géza Tóth, Carsten Klempt*

*Corresponding author. E-mail: klempt@iqo.uni-hannover.de

Published 27 April 2018, *Science* **360**, 416 (2017)
DOI: 10.1126/science.aao2035

This PDF file includes:

Supplementary Text:

Experimental sequence and analysis. The experimental procedure and evaluation, as well as a discussion of the number-dependent detection noise can be found in detail in the supplemental material of Ref. *(16)*.

We alternate between the experiments for the two measurement directions J_z and $J_\perp$ to minimize the influence of changing ambiance conditions. Both measurements start with the same experimental sequence. A BEC is prepared in a crossed-beam optical dipole trap in the state $F = 1, m_F = 0$.

A red-detuned microwave dressing field with a detuning of $206\,\mathrm{kHz}$ couples the levels $F = 1, m_F = -1$ and $F = 2, m_F = -2$. This induces an energy shift of the levels such that a resonance condition for spin-changing collisions from $F = 1, m_F = 0$ to $F = 1, m_F = \pm 1$ is reached *(16)*. At the resonance, the energy of two atoms in the $m_F = 0$ state is equal to the energy of two atoms in $m_F = \pm 1$ plus the energy of the excitation to the first spatially excited mode. This pair creation process, producing a pair of entangled atoms in $m_F = \pm 1$, is subject to bosonic enhancement, creating further pairs in the same mode during an interaction time of $t = 180\,\mathrm{ms}$. Due to the nature of the spin-changing collisions, the $F = 1, m_F = \pm 1$ levels are populated with a two-mode squeezed state. The two-mode squeezed state consists of a superposition of twin-Fock states $\sum_n c_n \left|n\right\rangle_{+1} \left|n\right\rangle_{-1}$ with an equal number of atoms $N_{\pm 1}$ in the two Zeeman levels $m_F = \pm 1$. The weight $c_n = \frac{(-i \tanh \xi)^n}{\cosh \xi}$ corresponds to a squeezing strength $\xi = \Omega t$ and a spin dynamics rate $\Omega = 2\pi \times 6.6\,\mathrm{Hz}$. The final measurement of the total number of atoms collapses the state onto a twin-Fock state. The measurement of J_z is now a measurement of the atom numbers in the two levels $m_F = \pm 1$ of the $F = 1$ manifold. However, to keep the two experimental procedures as similar as possible, the ensembles are transferred to the $F = 2$ manifold before detection. To this end, the pulse sequence of the transfer pulses

(II-IV) is reversed for the J_z measurements with respect to the $J_\perp$ measurement (see Fig. S1).

The measurement in the orthogonal direction requires a rotation around an axis perpendicular to J_z. This is achieved by a coupling of the ensembles in $F = 1, m_F = \pm 1$ by an effective $\pi/2$ pulse. Since the microwave phase is not synchronized to the atomic phases, the rotation leads to a measurement of $J_\perp$ along an arbitrary direction in the $x - y$ plane. However, the state is fully characterized due to its perfect symmetry under rotations around the z axis. Firstly, an ideal twin-Fock state is symmetric itself, and secondly, the experimentally realized state is randomized over J_z rotations due to the influence of magnetic field noise. Therefore, the measurement of $J_\perp$ is sufficient. The detection is again realized in the $F = 2$ manifold with the $m_F = \pm 1$ ensembles occupying $F = 2, m_F = -2$ and $F = 2, m_F = 0$. The large condensate from $m_F = 0$ is mainly transferred to $F = 2, m_F = -1$ with a small fraction transferred to $F = 2, m_F = 1$.

The experimental sequence ends with the detection of the atomic ensembles. The dipole trap is switched off to allow for $7.5\,\mathrm{ms}$ of self-similar expansion. The mode profiles remain undistorted but magnified due to the interaction of the ensembles with the large condensate remaining in the $F = 2, m_F = -1$ state *(40)*. After the initial mean-field dominated expansion, a strong magnetic field gradient is applied to spatially separate the atoms in the populated Zeeman levels. Finally, the number of atoms in the clouds is detected by absorption imaging on a CCD camera with a large quantum efficiency.

The absorption images are used to detect the number of atoms in the two spatially separated clouds. The center of mass of the large condensate in the $F = 2, m_F = -1$ level is used as a reference for the position of all clouds (see Fig. S1B). This is necessary due to slight shot-to-shot variations of the position, which result from minute position changes of the dipole trap. The position of the masks for the ensembles in $F = 2, m_F = \{-2, 0\}$ (formerly $F = 1, m_F = \pm 1$), as well as the cutting line for the parts a (left) and b (right), is fixed with respect to this reference.

The number of atoms in the four resulting sub-masks is then obtained by summing over the column density of the absorption image. The detection noise amounts on average to 24 atoms. It is independent of the particular number and is obtained by simultaneously evaluating empty images. The squeezed variance $(\Delta J_{\mathrm{z}})^2$ is calculated by subtracting the detection noise variance from the raw atomic variance.

To utilize the created state for quantum information tasks, it can be transferred into an optical lattice, where all constituent particles are individually addressable. As a concrete example, single-atom projective measurements on one half of this highly entangled ensemble allow to synthesize any pure symmetric quantum state in the second half *(35,36)*.

Bootstrapping. The error bars in Figs. 3 and 4 are obtained via a bootstrapping method. We created $10,000$ random data sets on the basis of the distributions of the experimental data. We then calculated the standard deviations of the measured quantities from these $10,000$ samples and checked that the percentage of violations of equation (1) was consistent with the reported significance.

Proof of equation (1). We start from the sum of two Heisenberg uncertainty relations $(\Delta J_{\mathrm{z}})^2[(\Delta J_{\mathrm{x}})^2+(\Delta J_{\mathrm{y}})^2] \geq \frac{1}{4}(\langle J_{\mathrm{x}}\rangle^2+\langle J_{\mathrm{y}}\rangle^2)$. Simple algebra yields

$$\left[(\Delta J_{\mathrm{z}})^2+\frac{1}{4}\right]\times\frac{(\Delta J_{\mathrm{x}})^2+(\Delta J_{\mathrm{y}})^2}{\langle J_{\mathrm{x}}^2\rangle+\langle J_{\mathrm{y}}^2\rangle}\geq\frac{1}{4}. \tag{S1}$$

Here, the first factor represents the fluctuations in the particle number difference and the second term represents the fluctuations in the phase difference.

Product states. First, we consider product states of the form $|\Psi^{(\mathrm{a})}\rangle\otimes|\Psi^{(\mathrm{b})}\rangle$. For such states

$$\begin{aligned}\left[(\Delta J_{\mathrm{z}}^{+})^2+\frac{1}{2}\right]&\times\left[(\Delta\tilde{J}_{\mathrm{x}}^{-})^2+(\Delta\tilde{J}_{\mathrm{y}}^{-})^2\right]\\&=[(\mathcal{U}^{(\mathrm{a})}+\tfrac{1}{4})+(\mathcal{U}^{(\mathrm{b})}+\tfrac{1}{4})]\cdot(\mathcal{V}^{(\mathrm{a})}+\mathcal{V}^{(\mathrm{b})})\\&\geq 4\sqrt{(\mathcal{U}^{(\mathrm{a})}+\tfrac{1}{4})(\mathcal{U}^{(\mathrm{b})}+\tfrac{1}{4})\mathcal{V}^{(\mathrm{a})}\mathcal{V}^{(\mathrm{b})}}\geq 1\end{aligned} \tag{S2}$$

holds, where we used the notation $\mathcal{U}^{(n)} = (\Delta J_{\rm z}^{(n)})^2$ and $\mathcal{V}^{(n)} = (\Delta \tilde{J}_{\rm x}^{(n)})^2 + (\Delta \tilde{J}_{\rm y}^{(n)})^2$ for $n = {\rm a}, {\rm b}$. For product states, the variance of a collective observable is the sum of the subsystem variances, i.e. $[\Delta(A^{({\rm a})} + A^{({\rm b})})]^2 = (\Delta A^{({\rm a})})^2 + (\Delta A^{({\rm b})})^2$, leading to the equality in equation (S2). The first inequality is obtained from the inequality between the arithmetic and the geometric mean. Equation (S1) is valid for both part ${\rm a}$ and ${\rm b}$ of the state, leading to the second inequality.

Using $\langle (\tilde{J}_{\rm x}^{(n)})^2 \rangle + \langle (\tilde{J}_{\rm y}^{(n)})^2 \rangle = 1$ for $n = {\rm a}, {\rm b}$, equation (S2) yields

$$2\left[(\Delta J_{\rm z}^{+})^2 + \frac{1}{2}\right](\mathcal{S} - \mathcal{C}) \geq \mathcal{S}, \tag{S3}$$

where correlations between the two subsystems are characterized by $\mathcal{C} = \left\langle \frac{J_{\rm x}^{({\rm a})} J_{\rm x}^{({\rm b})} + J_{\rm y}^{({\rm a})} J_{\rm y}^{({\rm b})}}{j_{\rm a} j_{\rm b}} \right\rangle$, and $\mathcal{S} = \mathcal{J}^{({\rm a})} \mathcal{J}^{({\rm b})}$. Note that $\mathcal{C}$ can be negative and $|\mathcal{C}| \leq \mathcal{S}$. The normalization with the total spin will make it easier to adapt our criterion to experiments with a varying particle number in the ensembles.

Separable states. We now consider a mixed separable state of the form $\varrho_{\rm sep} = \sum_k p_k |\Psi_k^{({\rm a})}\rangle \otimes |\Psi_k^{({\rm b})}\rangle$. For such states, we can write the following series of inequalities

$$\begin{aligned}
&2\left[(\Delta J_{\rm z}^{+})^2 + \frac{1}{2}\right](\mathcal{S} - \mathcal{C}) \\
&\quad \geq 2\left[\sum_k p_k (\Delta J_{\rm z})_k^2 + \frac{1}{2}\right]\left[\sum_k p_k \left(\mathcal{S}_k - \mathcal{C}_k\right)\right] \\
&\quad \geq 2\left[\sum_k p_k \sqrt{\left((\Delta J_{\rm z})_k^2 + \frac{1}{2}\right)\left(\mathcal{S}_k - \mathcal{C}_k\right)}\right]^2 \\
&\quad \geq \left(\sum_k p_k \sqrt{\mathcal{S}_k}\right)^2,
\end{aligned} \tag{S4}$$

where the subscript k indicates that the quantity is computed for the $k^{\rm th}$ sub-ensemble $|\Psi_k^{({\rm a})}\rangle \otimes |\Psi_k^{({\rm b})}\rangle$. The first inequality in equation (S4) is due to $(\Delta J_z^{+})^2$ and $\mathcal{S}$ being concave in the quantum state. The second inequality is based on the Cauchy-Schwarz inequality $\left(\sum_k p_k a_k\right)\left(\sum_k p_k b_k\right) \geq$

$\left(\sum_k p_k \sqrt{a_k b_k}\right)^2$, where $a_k, b_k \geq 0$. The third inequality is the application of equation (S3) for all sub-ensembles. Next, we find a lower bound on the RHS of equation (S4) based on the knowledge of $\mathcal{J}^{(\mathrm{a})}$ and $\mathcal{J}^{(\mathrm{b})}$. We find that

$$\sum_k p_k \left(\mathcal{J}_k^{(\mathrm{a})} \mathcal{J}_k^{(\mathrm{b})}\right)^{1/2} \geq (\mathcal{J}^{(\mathrm{a})})^2 + (\mathcal{J}^{(\mathrm{b})})^2 - 1, \tag{S5}$$

which is based on noting $(xy)^{1/4} \geq x + y - 1$ for $0 \leq x, y \leq 1$. Using equation (S5) to bound the RHS of equation (S4) from below and dividing by $\mathcal{S}$ we obtain

$$\left[(\Delta J_{\mathrm{z}}^{+})^2 + \frac{1}{2}\right] \times \left[2 - 2\frac{\mathcal{C}}{\mathcal{S}}\right] \geq \frac{\left[(\mathcal{J}^{(\mathrm{a})})^2 + (\mathcal{J}^{(\mathrm{b})})^2 - 1\right]^2}{\mathcal{S}}. \tag{S6}$$

Non-zero particle number variance. So far, we assumed that the particle number of the two clouds a and b are known constants. In practice, the particle number is not a constant, but varies from experiment to experiment. In principle, one could postselect experiments for a given particle number, and test entanglement only in the selected experiments. However, this leads to discarding most experiments, increasing the number of repetitions needed tremendously. Hence, we modify our condition to handle non-zero particle number variances *(41)*. In this case, the state of the system can be written as $\varrho = \sum_{j_{\mathrm{a}}, j_{\mathrm{b}}} Q_{j_{\mathrm{a}}, j_{\mathrm{b}}} \varrho_{j_{\mathrm{a}}, j_{\mathrm{b}}}$, where $\varrho_{j_{\mathrm{a}}, j_{\mathrm{b}}}$ are states with $2j_{\mathrm{a}}$ and $2j_{\mathrm{b}}$ particles in the two clouds, $Q_{j_{\mathrm{a}}, j_{\mathrm{b}}} \geq 0$, $\sum_{j_{\mathrm{a}}, j_{\mathrm{b}}} Q_{j_{\mathrm{a}}, j_{\mathrm{b}}} = 1$. The state ϱ is separable if and only if all ϱ_N are separable. Then, expectation values for ϱ are computed as $\langle A f(\hat{j}_{\mathrm{a}}, \hat{j}_{\mathrm{b}})\rangle_\varrho = \sum_{j_{\mathrm{a}}, j_{\mathrm{b}}} Q_{j_{\mathrm{a}}, j_{\mathrm{b}}} \langle A\rangle_{\varrho_{j_{\mathrm{a}}, j_{\mathrm{b}}}} f(j_{\mathrm{a}}, j_{\mathrm{b}})$, where the operator is separated into one part that depends only on the particle number operators of the two clouds represented by $\hat{j}_{\mathrm{a}}$ and $\hat{j}_{\mathrm{b}}$, and another part that does not depend on them. $f(x)$ denotes some function. The proof from equation (S2) to equation (S6) can then be repeated, assuming that j_{a} and j_{b} are operators. Hence, we arrive at the criterion that can be used for the case of varying particle numbers given in equation (1).

Note that we choose the normalization of the variances such that the criterion is robust against fluctuations of the total number of particles. For a constant particle number one could

simplify the fractions on the LHS of equation (1) by multiplying both the denominator and the numerator by j_{a}, and for the other fractions by j_{b}.

Supplementary figures

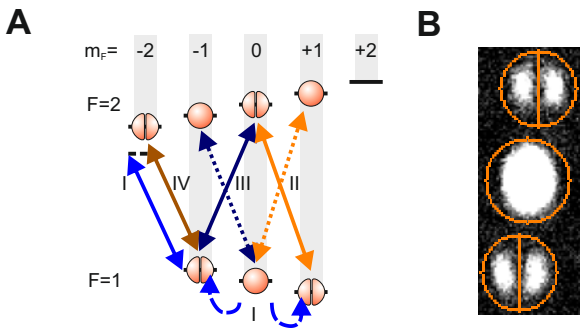

Figure S1: **Experimental techniques. (A)** Experimental procedure for the measurement of $J_\perp$. The sequence starts with a BEC in the $|F = 1, m_F = 0\rangle$ Zeeman level. (I) A microwave dressing field (solid blue line) induces a resonance condition for spin-changing collisions, allowing for the population of the $|1, \pm 1\rangle$ levels with a twin-Fock state (dashed blue line). (II) The population in $|1, 1\rangle$ is completely transferred to $|2, 0\rangle$ via a microwave transfer (solid orange arrows). This also leads to a population of $|2, 1\rangle$ with atoms from $|1, 0\rangle$ (dotted orange line). (III) A coupling between the two levels populated by the twin-Fock state is induced by a $\pi/2$ microwave pulse (solid dark blue line). This coupling is also resonant to the transition $|1, 0\rangle \rightarrow |2, -1\rangle$, populating the $|2, -1\rangle$ level (dotted dark blue line). (IV) To avoid an overlap in the detection of the atoms in $|1, -1\rangle$ and $|2, 1\rangle$ the ensemble from $|1, -1\rangle$ is transferred to $|2, -2\rangle$ (solid dark orange line). **(B)** Single-shot absorption image with read-out masks indicated in orange. The position of the masks is determined by the center of mass of the central atomic cloud. The other two masks, as well as the cutting lines, are fixed with respect to the central cloud. The atom numbers in all four sub-masks are evaluated by summing over the column densities in the appropriate sub-masks.

References and Notes

1. T. Monz, P. Schindler, J. T. Barreiro, M. Chwalla, D. Nigg, W. A. Coish, M. Harlander, W. Hänsel, M. Hennrich, R. Blatt, 14-Qubit entanglement: Creation and coherence. *Phys. Rev. Lett.* **106**, 130506 (2011). doi:10.1103/PhysRevLett.106.130506 Medline

2. R. Islam *et al.*, *Nature* **528**, 77–83 (2015).

3. X.-L. Wang, L.-K. Chen, W. Li, H.-L. Huang, C. Liu, C. Chen, Y.-H. Luo, Z.-E. Su, D. Wu, Z.-D. Li, H. Lu, Y. Hu, X. Jiang, C.-Z. Peng, L. Li, N.-L. Liu, Y.-A. Chen, C.-Y. Lu, J.-W. Pan, Experimental ten-photon entanglement. *Phys. Rev. Lett.* **117**, 210502 (2016). doi:10.1103/PhysRevLett.117.210502 Medline

4. R. McConnell, H. Zhang, J. Hu, S. Ćuk, V. Vuletić, Entanglement with negative Wigner function of almost 3,000 atoms heralded by one photon. *Nature* **519**, 439–442 (2015). doi:10.1038/nature14293 Medline

5. F. Haas, J. Volz, R. Gehr, J. Reichel, J. Estève, Entangled states of more than 40 atoms in an optical fiber cavity. *Science* **344**, 180–183 (2014). doi:10.1126/science.1248905 Medline

6. O. Hosten, N. J. Engelsen, R. Krishnakumar, M. A. Kasevich, Measurement noise 100 times lower than the quantum-projection limit using entangled atoms. *Nature* **529**, 505–508 (2016). doi:10.1038/nature16176 Medline

7. B. Julsgaard, A. Kozhekin, E. S. Polzik, Experimental long-lived entanglement of two macroscopic objects. *Nature* **413**, 400–403 (2001). doi:10.1038/35096524 Medline

8. J. Estève, C. Gross, A. Weller, S. Giovanazzi, M. K. Oberthaler, Squeezing and entanglement in a Bose-Einstein condensate. *Nature* **455**, 1216–1219 (2008). doi:10.1038/nature07332 Medline

9. C. Gross, T. Zibold, E. Nicklas, J. Estève, M. K. Oberthaler, Nonlinear atom interferometer surpasses classical precision limit. *Nature* **464**, 1165–1169 (2010). doi:10.1038/nature08919 Medline

10. M. F. Riedel, P. Böhi, Y. Li, T. W. Hänsch, A. Sinatra, P. Treutlein, Atom-chip-based generation of entanglement for quantum metrology. *Nature* **464**, 1170–1173 (2010). doi:10.1038/nature08988 Medline

11. B. Lücke, M. Scherer, J. Kruse, L. Pezzé, F. Deuretzbacher, P. Hyllus, O. Topic, J. Peise, W. Ertmer, J. Arlt, L. Santos, A. Smerzi, C. Klempt, Twin matter waves for interferometry beyond the classical limit. *Science* **334**, 773–776 (2011). doi:10.1126/science.1208798 Medline

12. C. D. Hamley, C. S. Gerving, T. M. Hoang, E. M. Bookjans, M. S. Chapman, Spin-nematic squeezed vacuum in a quantum gas. *Nat. Phys.* **8**, 305–308 (2012). doi:10.1038/nphys2245

13. T. Berrada, S. van Frank, R. Bücker, T. Schumm, J.-F. Schaff, J. Schmiedmayer, Integrated Mach-Zehnder interferometer for Bose-Einstein condensates. *Nat. Commun.* **4**, 2077 (2013). doi:10.1038/ncomms3077 Medline

14. N. Killoran, M. Cramer, M. B. Plenio, Extracting entanglement from identical particles. *Phys. Rev. Lett.* **112**, 150501 (2014). doi:10.1103/PhysRevLett.112.150501 Medline

15. B. Yurke, D. Stoler, Bell's-inequality experiments using independent-particle sources. *Phys. Rev. A* **46**, 2229–2234 (1992). doi:10.1103/PhysRevA.46.2229 Medline

16. B. Lücke, J. Peise, G. Vitagliano, J. Arlt, L. Santos, G. Tóth, C. Klempt, Detecting multiparticle entanglement of Dicke states. *Phys. Rev. Lett.* **112**, 155304 (2014). doi:10.1103/PhysRevLett.112.155304 Medline

17. X.-Y. Luo, Y.-Q. Zou, L.-N. Wu, Q. Liu, M.-F. Han, M. K. Tey, L. You, Deterministic entanglement generation from driving through quantum phase transitions. *Science* **355**, 620–623 (2017). doi:10.1126/science.aag1106 Medline

18. J. Peise, I. Kruse, K. Lange, B. Lücke, L. Pezzè, J. Arlt, W. Ertmer, K. Hammerer, L. Santos, A. Smerzi, C. Klempt, Satisfying the Einstein-Podolsky-Rosen criterion with massive particles. *Nat. Commun.* **6**, 8984 (2015). doi:10.1038/ncomms9984 Medline

19. J. Tura, R. Augusiak, A. B. Sainz, T. Vértesi, M. Lewenstein, A. Acín, Quantum nonlocality. Detecting nonlocality in many-body quantum states. *Science* **344**, 1256–1258 (2014). doi:10.1126/science.1247715 Medline

20. J. Tura, R. Augusiak, A. B. Sainz, B. Lücke, C. Klempt, M. Lewenstein, A. Acín, Nonlocality in many-body quantum systems detected with two-body correlators. *Ann. Phys.* **362**, 370–423 (2015). doi:10.1016/j.aop.2015.07.021

21. R. Schmied, J.-D. Bancal, B. Allard, M. Fadel, V. Scarani, P. Treutlein, N. Sangouard, Bell correlations in a Bose-Einstein condensate. *Science* **352**, 441–444 (2016). doi:10.1126/science.aad8665 Medline

22. R. Bücker, J. Grond, S. Manz, T. Berrada, T. Betz, C. Koller, U. Hohenester, T. Schumm, A. Perrin, J. Schmiedmayer, Twin-atom beams. *Nat. Phys.* **7**, 608–611 (2011). doi:10.1038/nphys1992

23. R. Lopes, A. Imanaliev, A. Aspect, M. Cheneau, D. Boiron, C. I. Westbrook, Atomic Hong-Ou-Mandel experiment. *Nature* **520**, 66–68 (2015). doi:10.1038/nature14331 Medline

24. P. Dussarrat, M. Perrier, A. Imanaliev, R. Lopes, A. Aspect, M. Cheneau, D. Boiron, C. I. Westbrook, Two-particle four-mode interferometer for atoms. *Phys. Rev. Lett.* **119**, 173202 (2017). doi:10.1103/PhysRevLett.119.173202 Medline

25. C. Klempt, O. Topic, G. Gebreyesus, M. Scherer, T. Henninger, P. Hyllus, W. Ertmer, L. Santos, J. J. Arlt, Multiresonant spinor dynamics in a Bose-Einstein condensate. *Phys. Rev. Lett.* **103**, 195302 (2009). doi:10.1103/PhysRevLett.103.195302 Medline

26. M. Scherer, B. Lücke, G. Gebreyesus, O. Topic, F. Deuretzbacher, W. Ertmer, L. Santos, J. J. Arlt, C. Klempt, Spontaneous breaking of spatial and spin symmetry in spinor condensates. *Phys. Rev. Lett.* **105**, 135302 (2010). doi:10.1103/PhysRevLett.105.135302 Medline

27. J. DiGuglielmo, B. Hage, A. Franzen, J. Fiurášek, R. Schnabel, Experimental characterization of gaussian quantum-communication channels. *Phys. Rev. A* **76**, 012323 (2007). doi:10.1103/PhysRevA.76.012323

28. T. Eberle, V. Händchen, J. Duhme, T. Franz, R. F. Werner, R. Schnabel, Strong einstein-podolsky-rosen entanglement from a single squeezed light source. *Phys. Rev. A* **83**, 052329 (2011). doi:10.1103/PhysRevA.83.052329

29. A. Einstein, B. Podolsky, N. Rosen, Can quantum-mechanical description of physical reality be considered complete? *Phys. Rev.* **47**, 777–780 (1935). doi:10.1103/PhysRev.47.777

30. L.-M. Duan, G. Giedke, J. I. Cirac, P. Zoller, Inseparability criterion for continuous variable systems. *Phys. Rev. Lett.* **84**, 2722–2725 (2000). doi:10.1103/PhysRevLett.84.2722 Medline

31. R. Simon, Peres-horodecki separability criterion for continuous variable systems. *Phys. Rev. Lett.* **84**, 2726–2729 (2000). doi:10.1103/PhysRevLett.84.2726 Medline

32. Materials and methods are available as supplementary materials.

33. M. D. Reid, Demonstration of the Einstein-Podolsky-Rosen paradox using nondegenerate parametric amplification. *Phys. Rev. A* **40**, 913–923 (1989). doi:10.1103/PhysRevA.40.913 Medline

34. L.-M. Duan, A. Sørensen, J. I. Cirac, P. Zoller, Squeezing and entanglement of atomic beams. *Phys. Rev. Lett.* **85**, 3991–3994 (2000). doi:10.1103/PhysRevLett.85.3991 Medline

35. W. Wieczorek, R. Krischek, N. Kiesel, P. Michelberger, G. Tóth, H. Weinfurter, Experimental entanglement of a six-photon symmetric Dicke state. *Phys. Rev. Lett.* **103**, 020504 (2009). doi:10.1103/PhysRevLett.103.020504 Medline

36. N. Kiesel, W. Wieczorek, S. Krins, T. Bastin, H. Weinfurter, E. Solano, Operational multipartite entanglement classes for symmetric photonic qubit states. *Phys. Rev. A* **81**, 032316 (2010). doi:10.1103/PhysRevA.81.032316

37. F. Laloë, W. J. Mullin, Interferometry with independent Bose-Einstein condensates: Parity as an EPR/Bell quantum variable. *Eur. Phys. J. B* **70**, 377–396 (2009). doi:10.1140/epjb/e2009-00248-6

38. P. Kunkel, M. Prüfer, H. Strobel, D. Linnemann, A. Frölian, T. Gasenzer, M. Gärttner, M. K. Oberthaler, Spatially distributed multipartite entanglement enables EPR steering of atomic clouds. *Science* **360**, 413–416 (2018).

39. M. Fadel, T. Zibold, B. Décamps, P. Treutlein, Spatial entanglement patterns and Einstein-Podolsky-Rosen steering in Bose-Einstein condensate. *Science* **360**, 409–413 (2018).

40. Y. Castin, R. Dum, Bose-Einstein condensates in time dependent traps. *Phys. Rev. Lett.* **77**, 5315–5319 (1996). doi:10.1103/PhysRevLett.77.5315 Medline

41. P. Hyllus, L. Pezzé, A. Smerzi, G. Tóth, Entanglement and extreme spin squeezing for a fluctuating number of indistinguishable particles. *Phys. Rev. A* **86**, 012337 (2012). doi:10.1103/PhysRevA.86.012337